Available online at www.sciencedirect.com
SCIENCE DIRECT
Polymer 47 (2006) 2728–2740
polymer
www.elsevier.com/locate/polymer

Sorption of iodine by polyurethane and melamine-formaldehyde foams using iodine sublimation and iodine solutions

Yanbing Wang [a], Gregory A. Sotzing [a,b,*], R.A. Weiss [a,c,**]

[a] Polymer Science Program, University of Connecticut, Storrs, CT 06269-3136, USA
[b] Department of Chemistry, University of Connecticut, Storrs, CT 06269-3136, USA
[c] Department of Chemical Engineering, University of Connecticut, Storrs, CT 06269-3136, USA

Received 9 December 2005; received in revised form 17 February 2006; accepted 20 February 2006
Available online 14 March 2006

Abstract

Iodine sorption by polyurethane (PU) and melamine-formaldehyde (MF) foams was studied using both iodine sublimation and iodine solutions with hexanes and toluene. In the sublimation process, the diffusion kinetics was investigated and the interaction between iodine and PU foams was characterized by DSC, TGA, Raman spectroscopy and electrical conductivity measurements. In the solution process, the equilibrium absorption followed the distribution law and the distribution coefficients varied depending on the solvent used. MF foam achieved no iodine absorption in both processes which can be attributed to the lack of charge–transfer interactions.

Keywords: Anomalous diffusion; Distribution law; Charge–transfer interaction

1. Introduction

The diffusion of small molecules in polymers is important in many areas of polymer technology such as packaging of foods, drugs, and cosmetics, controlled release of dissolved materials, treatment of waste waters, chromatographic analysis, and separation of gases [1–3]. The preparation of conductive polymer blends is a new technology which benefits from the diffusion in polymers. Conductive polymers have been the focus of considerable research over the past two decades with foreseeable use in products such as rechargeable batteries, bio- and chemical-sensors, transducers, antistatic coatings, and EMI shielding materials [4,5]. Polypyrrole (PPy) is one of the most stable conductive polymers due to its heterocyclic structure [6], though neat PPy is an intractable, brittle solid, which greatly hampers its application. One approach for exploiting the intrinsic electrical conductivity of PPy and overcoming its poor mechanical properties is to blend it with an insulating host polymer with better mechanical properties. Conductive blends may be prepared by impregnating the host polymer first with pyrrole and then with an oxidant, or by treating an oxidant-doped polymer with a pyrrole solution or vapor, which results in the in situ polymerization of pyrrole within the host polymer [5,7]. Most research on PPy/polymer blends has focused on the properties of the resultant conductive blends. The frequently overlooked fact, however, is that the polymerization of pyrrole occurs only in the presence of the oxidant. Therefore, the oxidant impregnation process and the interactions between the oxidant and the host polymer determine the amount of PPy produced and how it is distributed within the host polymer.

Several methods have been employed to incorporate oxidants into host polymers. The most typical method is to swell the host polymer with an oxidant solution and allow the host polymer to absorb the oxidant. Fu et al. [8] used $FeCl_3$/methanol solutions to incorporate $FeCl_3$ into polyurethane (PU) foams with three different densities. The absorption equilibrium was achieved in less than 5 h. For each foam the $FeCl_3$ mass uptake increased linearly with increasing oxidant solution concentration, and for a fixed $FeCl_3$ solution concentration, the $FeCl_3$ mass uptake increased with decreasing PU foam density. Ishizu et al. [9,10] crosslinked and quaternized poly(styrene-*b*-2-vinylpyridine) (PS2VP) to increase the hydrophilicity of the P2VP microdomains, and then used dioxane/water mixed solvents to incorporate the

* Corresponding authors. Address: Department of Chemistry, Institute of Materials Science, University of Connecticut, Storrs, CT 06269-3136, USA. Tel.: +1 860 486 4619; fax: +1 860 486 4745.
** Address: Department of Chemical Engineering, University of Connecticut, Storrs, CT 06269-3136, USA. Tel.: +1 860 486 4698; fax: +1 860 486 4745.
E-mail addresses: sotzing@mail.ims.uconn.edu (G.A. Sotzing), rweiss@mail.ims.uconn.edu (R.A. Weiss).

0032-3861/$ - see front matter © 2006 Elsevier Ltd. All rights reserved.
doi:10.1016/j.polymer.2006.02.063

oxidant $CuCl_2$ into the host PS2VP. TEM micrographs showed that Cu^{2+} ions were distributed only in the nanometer-sized spherical microdomains of P2VP and complexed with the pyridine nitrogens; the ionic complex concentration increased with increasing dioxane fraction in the mixed solvent. A second method was also employed by Ishizu et al. [10] in which both PS2VP and $CuCl_2$ were dissolved in the mixed solvents and then polymer films were cast and quaternized. TEM micrographs showed the same distribution of the ionic complex as was achieved by the previous method, though the second method had the advantage that the amount of Cu^{2+} ions introduced could be quantitatively controlled by changing the amount of $CuCl_2$ in the feed. Lafosse [11] described an oxidant sorption method for the synthesis of PPy/PTFE blends. A surfactant stabilized PTFE emulsion was mixed with aqueous ferric *para*-toluenesulfonate solution. Pyrrole was then added to produce a PPy/PTFE blend. It was presumed that the blend consisted of PTFE spherical grains partially covered by a PPy layer. Zoppi et al. [12] prepared PPy/EPDM blends by first mechanically mixing $CuCl_2$ into EPDM rubber, and then exposing the EPDM containing $CuCl_2$ to pyrrole vapor. The PPy weight fraction in the blend increased with decreasing oxidant particle size.

Two new methods for incorporating oxidants into host polymers were recently developed in our laboratory to eliminate the use of large amounts of volatile organic compounds (VOC) as solvents. The first one was to use supercritical carbon dioxide ($scCO_2$) as the solvent [13–15]. That procedure produced Fickian diffusion of ferric triflate into PU foams [13]. But the oxidant, and hence, the resultant PPy, were restricted to a relatively thin layer near the surface of the foam. The poor penetration was thought to be due to the low solubility of ferric triflate in $scCO_2$ and the inability of $scCO_2$ to significantly swell the PU. Small amounts of ethanol cosolvent improved both the ferric triflate solubility and the PU swelling, which resulted in faster diffusion kinetics, better penetration, and a more uniform distribution of ferric triflate in the PU foams [14]. The degree of improvement increased with increasing ethanol concentration. Ferric trifluoroacetate was also incorporated into the PU foams using $scCO_2$/ethanol as the solvent [14]. It had a higher solubility in $scCO_2$ than ferric triflate, but produced a lower concentration of the oxidant in the PU foams. The sorption equilibria of iodine in PU foams using $scCO_2$ as a solvent was also studied [15]. Linear sorption isotherms were obtained, and the distribution coefficients of iodine between the PU foam and the $scCO_2$ solutions were determined. The second method of oxidant impregnation was by the sublimation of iodine [16,17]. The iodine sorption by PU foams followed Fickian kinetics and the sorption rate increased with increasing temperature [16].

The main objective of this paper was to investigate the sorption of iodine oxidant by host polymers based on the interactions between iodine and the polymers. The iodine sorption by three PU foams and one melamine-formaldehyde (MF) foam using both iodine sublimation and iodine solutions was studied. In the iodine sublimation process, the sorption kinetics was analyzed considering mass transfer models and interactions between iodine and the host polymers. The effects of temperature and foam structure were also investigated. For the iodine solution process, the sorption kinetics and equilibria were studied and the equilibria were explained by a distribution law based on the interactions between polymers, iodine, and solvents. The effects of solvents and foam structure were also investigated for that method.

2. Experimental

2.1. Materials

Three different polyurethane (PU) foams and one melamine-formaldehyde (MF) foam were obtained from McMaster-Carr Supply Company. All the foams were white, skin-free, and had an open-cell structure. The PU foams were lightly crosslinked elastomers made from 2,6-toluene diisocyanate (TDI) and polyether polyols. The three PU foams are referred to as PU1, PU2, and PU3, respectively, according to their firmness rating numbers—PU1 having the lowest crosslinking density and lowest modulus of the three PUs. The foam sample was cut to a size of $2.5\times2.5\times1.3$ cm and extracted with acetone before use. The extraction was done to remove any additives to the foam that may be subsequently extracted during the procedures used for preparing the conductive foams. That removed any ambiguity from the mass balances used to determine the iodine absorption and the amount of conductive polymer produced. The acetone extracted less than 10 wt% of the foam, and subsequent extractions with toluene or hexanes did not remove any additional mass. Iodine (p.a.) from ACROS was used as received. Reagent grade toluene, hexanes, and acetone were obtained from Fisher Scientific and used as received.

2.2. Iodine sublimation process

The foam sample was impregnated with iodine by placing the foam in a desiccator containing iodine, taking care not to allow contact between the foam and the iodine crystals. The diffusion rate of iodine into the foam was controlled by varying the temperature by placing the desiccator in a convection oven. Three temperatures: 25, 40, and 70 °C, were used. After a specified sorption time, the foam was removed from the desiccator and weighed. The iodine concentration in the foam was calculated as weight percent (wt%) based on the mass of the original neat foam, i.e. wt% iodine = (mass of iodine/mass of foam before iodine loading) $\times$ 100%.

2.3. Iodine solution process

Iodine solutions with different concentrations were prepared in hexanes and toluene. Each foam sample was immersed in a 50 mL iodine solution of fixed concentration for ca. 2 h to swell the foam and allow iodine to diffuse into the foam. The sample was then removed from the solution and squeezed to remove the solvent. The resultant foam was dried for ca. 1 h to evaporate any remaining solvent and then weighed. The whole

iodine solution process was carried out at room temperature and atmospheric pressure. The iodine concentration in the foam was calculated as in the sublimation process.

2.4. Swelling measurements

Swelling measurements were made for the three PU foams in two solvents: hexanes and toluene. The thickness of a dried foam sample was first measured, and then the sample was immersed in solvent and allowed to equilibrate at room temperature. The thickness of the swelled sample was measured in the solvent. The precision of the thickness measurement was 0.002 cm, and the swelling ratio was calculated from Eq. (1)

$$\text{Swelling ratio} = \frac{t_{\text{wet}} - t_{\text{dry}}}{t_{\text{dry}}} \times 100 \quad (1)$$

where t_{dry} was the thickness of the dry sample and t_{wet} was the thickness of sample in the solvent. The swelling ratio of the iodine impregnated PU foam was also determined in the same manner.

2.5. Water sonication

The iodine impregnated PU foam was sonicated in 100 mL de-ionized water three times for 5 min each. The foam was then dried for ca. 4 h to evaporate remaining water and weighed to determine the iodine concentration (wt%) in the foam.

2.6. Materials characterization

The densities of the neat foams were calculated from the mass and volume of the sample after acetone extraction. Compression tests were performed using an Instron model 1011 with a 4.5 kg load cell and a crosshead speed of 0.635 cm/min. The compression modulus of elasticity was calculated as the initial slope ($<5\%$ strain) of the stress–strain curve. The fracture surface morphology of PU dense regions was characterized with a JEOL JSM-6335F field emission scanning electron microscope (SEM) on foam samples fractured after immersion in liquid nitrogen. Fourier transform infrared (FTIR) spectra were measured with a Nicolet 560 Magna-IR spectrometer. A Perkin–Elmer Lambda 900 UV spectrometer was used for UV/Vis measurements. The anti-Stoke Raman spectra of the iodine impregnated PU foams were recorded with a Renishaw Ramanoscope system using a 514.5 nm (2.41 eV) argon laser focused on a 1 μm spot by a 100× objective lens. DC conductivity measurements of iodine impregnated PU foams were made with a four-point fixture consisting of four parallel copper wires separated by 0.42 cm that were pressed onto one 2.54×2.54 cm surface of the foam sample. Slight pressure, just enough to assure a good contact between the foam sample and the electrodes, was applied. A constant current supplied by a Keithley 224 programmable current source was supplied through the outer wires, and the voltage drop across the inner wires was recorded with a Keithley 2700 multimeter. The measurements were made under ambient conditions.

Thermal stability of the foams was measured with a TA Instruments TGA-2950, using a nitrogen atmosphere and a heating rate of 10 °C/min. Differential scanning calorimetry (DSC) of iodine, neat foams, and iodine impregnated foams was performed with a TA Instruments DSC-2920 using a nitrogen atmosphere. Samples were quenched to about −100 °C using liquid nitrogen, and followed by a heating scan at 10 °C/min to 0 °C. T_g was defined as the midpoint of the change in the heat capacity at the transition (ΔC_p).

3. Results and discussion

3.1. Characterization of PU foams

Fig. 1 shows optical micrographs of the PU1, PU2, and PU3 foams in transmission. The open-cell structure is revealed in Fig. 1, and the morphology of the three foams was similar. The PU foam can be viewed as a three-dimensional network of PU fibers and air cells. The PU fiber size was about 70 μm and the air cell size range was 200–400 μm. Fracture surfaces of the PU1 and PU2 foams measured by SEM (not shown) were smooth, but there were large amounts of 0.2–1 μm particles on the fracture surface of the PU3 foams. The particles were believed to be inorganic fillers.

The mechanical properties and densities of the PU foams are summarized in Table 1. PU1 and PU2 have the same density, and PU3 has a higher density because of the inorganic fillers. The firmness rating of the PU foams is based on their compressive stress at 25% deflection, which increased from PU1 through PU2 to PU3. The compression modulus exhibits the same increasing tendency. PU1 and PU3 have the same reported tensile strength, while PU2 has the highest tensile strength.

TGA results using a nitrogen atmosphere for the PU foams are shown in Fig. 2. The foams lost less than 1% mass below 200 °C. A major degradation process occurred for all three foams between 250 and 400 °C. PU1 and PU2 showed no difference in their thermal degradation behavior and lost nearly 100% mass by 630 °C. About 40% mass remained for PU3 at 630 °C, and another major degradation process occurred between 630 and 800 °C. No further mass loss was observed for PU3 above 800 °C, and about 17% mass remained at 900 °C, which was due to the presence of inorganic fillers.

Rubber elasticity theory predicts that the elastic modulus is directly proportional to the crosslinking density, and the tensile strength is also expected to increase with increasing crosslinking density [18]. A higher crosslinking density is probably the reason that the PU2 foam had a higher compression modulus and tensile strength than the PU1 foam. Rigid particulate fillers in a polymer usually increase the modulus and decrease the tensile strength [18], and the higher compression modulus and lower tensile strength of PU3 foams compared with PU2 foams are consistent with the presence of inorganic fillers in the PU3 foam.

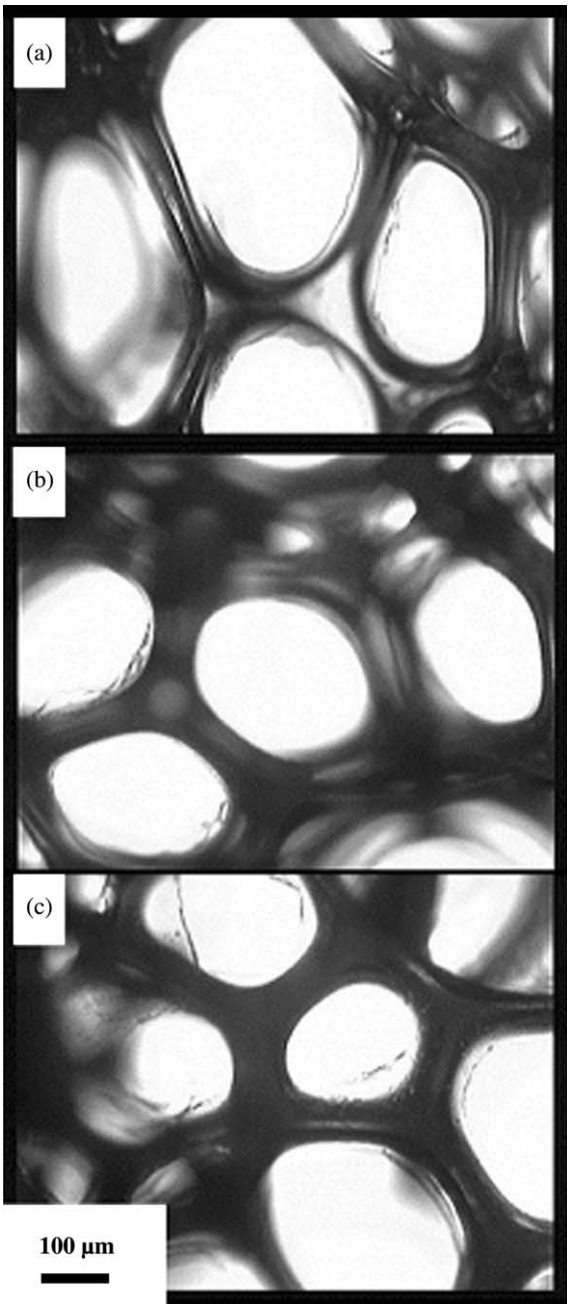

Fig. 1. Optical micrographs of (a) PU1, (b) PU2, and (c) PU3 foams in transmission mode.

DSC results for the PU foams are summarized in Table 2. Each foam exhibited a single, but broad glass transition in the temperature range from −100 to 0 °C. The T_g's of the three PU foams were similar, which indicates that they had similar chemical structures. The ΔC_p at the glass transition for the PU2 foam was slightly less than that for the PU1 foam. This is probably because of the higher crosslinking density of the PU2 foam, but the difference was not large enough to affect the T_g. The ΔC_p at the glass transition for the PU3 foam was significantly less than those for the PU1 and PU2 foams, which is consistent with the former material containing inorganic fillers, as concluded from the SEM and TGA results.

Table 1
Mechanical properties and density of PU foams

Foam	Compressive stress at 25% deflection[a] (kPa)	Tensile strength[a] (kPa)	Compression modulus (kPa)	Density (g/cm^3)
PU1	2.4	55	39.5 (1.6)[b]	0.045
PU2	4.8	62	63.6 (6.2)	0.045
PU3	6.2	55	85.2 (4.1)	0.059

[a] Data obtained from material specifications.
[b] The number in parentheses is the standard deviation of five measurements.

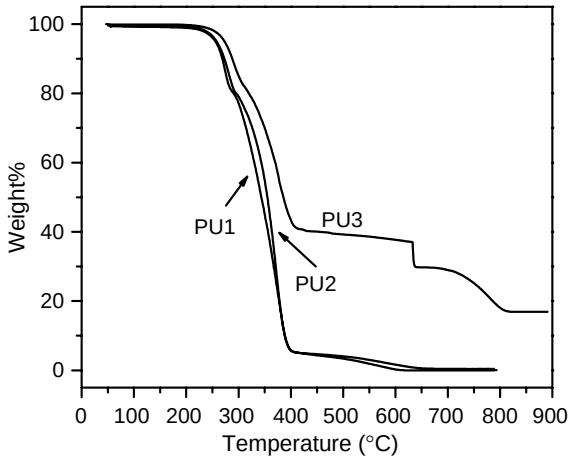

Fig. 2. TGA of PU1, PU2, and PU3 foams.

3.2. Iodine sublimation process

3.2.1. Diffusion models

The unidirectional, isothermal penetrant diffusion within a polymer film of thickness L is described by Fickian second law along with the appropriate initial and boundary conditions, which may be written as [19]

$$\frac{\partial C}{\partial t} = D\frac{\partial^2 C}{\partial x^2} \tag{2}$$

$$t = 0; \quad 0 < x < L; \quad C = 0 \tag{3}$$

$$t > 0; \quad x = 0, \quad x = L; \quad C = C_0 \tag{4}$$

Here, the diffusivity, D, is assumed to be a function only of temperature, C is the penetrant concentration within the polymer film at time t and distance x, and C_0 is the constant penetrant concentration at the surface of the polymer film. The solution to the Fickian diffusion equation is

$$\frac{M_t}{M_\infty} = 1 - \sum_{n=0}^{\infty} \frac{8}{(2n+1)^2\pi^2} \exp\left[\frac{-D(2n+1)^2\pi^2}{L^2} t\right] \tag{5}$$

Table 2
T_g and ΔC_p at the glass transition of PU foams

Foam	T_g onset (°C)	T_g midpoint (°C)	T_g end (°C)	ΔC_p (J/g/°C)
PU1	−56.1	−50.9	−45.8	0.498
PU2	−57.0	−51.5	−46.0	0.458
PU3	−56.8	−51.3	−45.8	0.236

where M_t and M_∞ are the penetrant mass uptakes at time t and at equilibrium. A widely used approximation is that at short time ($M_t/M_\infty < 0.5$), the penetrant mass uptake is proportional to $t^{1/2}$, which is given as

$$\frac{M_t}{M_\infty} = 4\left(\frac{Dt}{\pi L^2}\right)^{1/2} \tag{6}$$

D may be calculated from the slope of the initial linear portion of a plot of M_t/M_∞ versus $t^{1/2}$, or it can be estimated from the long-time approximation ($M_t/M_\infty > 0.4$),

$$\frac{M_t}{M_\infty} = 1 - \frac{8}{\pi^2}\exp\left(\frac{-D\pi^2}{L^2}t\right) \tag{7}$$

When the penetrant has a molecular size much smaller than the monomer unit of the polymer and the interaction between the two components is very weak, a limited rotational oscillation of only one or two monomer units would be sufficient to create openings for the penetrant molecule to jump thermally from one position to a neighboring one. The diffusion of simple gases, such as hydrogen, argon, and nitrogen, in an amorphous polymer matrix and of water in hydrophobic polymers probably involves such a molecular mechanism and shows typical Fickian diffusion behavior [19]. The diffusivity usually follows an Arrhenius relationship, characteristic of an activated process

$$D = D_0\exp\left(\frac{-E_D}{RT}\right) \tag{8}$$

Here, D_0 is a constant and E_D is the activation energy required to create an opening between polymer chains large enough to allow the penetrant molecule to pass, which can be described by various molecular models [2,20,21].

The Fickian model is the simplest diffusion model, but it is not valid in some cases. For the penetrant with a molecular size comparable with, or larger than, the monomer unit of the polymer, the diffusion process requires rearrangement of the polymer segments in order to accommodate the mass transport. This structural relaxation process can often dominate the overall diffusion kinetics. Such substances include most organic vapors, which are either solvents or swelling agents for ordinary polymers [19]. To investigate the mechanism of diffusion, kinetic results can be fitted to a power law equation [1,22]

$$\frac{M_t}{M_\infty} = kt^n \tag{9}$$

where k is a constant incorporating characteristics of the polymer-penetrant systems, t is time and the exponent n indicates the type of diffusion mechanism. $n = 0.5$ implies Fickian diffusion; $n = 1.0$ implies case II diffusion; and for $0.5 < n < 1.0$, anomalous diffusion occurs. Fickian diffusion ($n = 0.5$) is usually found for rubbery polymers where the structural relaxation is fast compared with the diffusion process. The diffusion rate decreases continuously with time, owing to the continuous decrease of the driving concentration gradient [23]. Case II diffusion ($n = 1.0$) is usually found for glassy polymers where the structural relaxation is slow compared with diffusion and becomes the rate-determining step. Case II diffusion is characterized by a sharp penetrant front advancing linearly with time and a uniform penetrant concentration in the polymer matrix [24,25]. Anomalous diffusion is a process with intermediate characteristics [26].

Diffusivity can be significantly influenced by small changes in the chemical structure of the penetrant-polymer system [27]. Diffusion of a relatively non-interacting penetrant in a polymer often follows Fickian behavior with a constant diffusivity. An increase in the interactions between the penetrant and polymer leads to an increased diffusion rate, and the diffusion process becomes concentration dependent and deviates from the Fickian model due to complicated relaxation effects. The relaxation might be accompanied by polymer swelling [2]. Fujita [28] extended the free-volume theory to account for the concentration dependence of diffusivity. This theory assumes that the diffusion rate depends primarily on the ease with which the polymer segments exchange their positions with penetrant molecules. The mobility of the polymer, in turn, depends on the amount of free-volume in the matrix and thus relates diffusivity to the fractional free-volume of a system. According to Fujita's theory, the diffusivity increases with increasing fractional free-volume at constant temperature. Schneider et al. [29] showed that the diffusion of toluene in butyl rubber followed Fujita's free-volume theory. The WLF equation, which is based on free-volume theory, successfully describes the temperature dependence of gas diffusivity in rubbery polymers [30]. Crank [31] also proposed a diffusion model based on polymer swelling in which the deviation from Fickian diffusion was attributed to the differential swelling stresses (DSS) generated by the constraints imposed on the outer, swelling part by the inner, less swelling part of the polymer. The stresses change as diffusion proceeds, since the concentration distribution in the polymer changes with time and the polymer chains tend to relieve the stresses by changing their conformations, which cause the diffusivity to be concentration and time dependent. Sanopoulou et al. [32] applied the DSS modeling approach successfully to the diffusion in methanol–cellulose acetate system.

3.2.2. Initial adsorption process

In the sublimation process, saturated iodine vapor filled the desiccator. The vapor pressure of iodine at different temperatures can be calculated according to the equation [33]

$$\log p = 13.374 - \frac{3512.8}{T} - 2.013\log T \tag{10}$$

where p is the saturated vapor pressure of the iodine crystals in atm and T is the temperature in K. The vapor pressure at 25, 40, and 70 °C was 41, 136, and 1083 Pa, respectively. After a PU foam was placed in the desiccator filled with iodine vapor, the color of the foam changed gradually from white to yellow to brown and finally to black. The color change occurred at the initial stage of diffusion and the changes were faster at higher temperature. Visual observation found that the distribution of iodine from the surface to the core of the foam was

homogeneous for the samples with an iodine concentration higher than 10 wt%. At the later stage of diffusion, a lustrous glow from tiny iodine crystals were observed for some samples, which suggests that the iodine precipitated and crystallized in the foam pores once the polymer dense regions became saturated. The rate of adsorption is typically much faster than the rate of diffusion [34]. We expect that the open cells of the foam quickly became saturated with iodine vapor and an adsorption equilibrium was established at the initial stage of permeation of the iodine in the foam, so that diffusion dominated the overall mass transfer. The amount of iodine adsorbed at equilibrium can be considered the penetrant concentration at the surface of the polymer dense fibers, C_0, in the boundary condition in Eq. (4). In the Fickian model, the change in C_0 does not affect diffusivity D, but affects M_∞. The equilibrium adsorption is usually modeled by isotherms, and the most commonly used isotherm in this regard is the Freundlich isotherm [34,35]

$$C_{ad} = kp^n \tag{11}$$

where C_{ad} is the amount of iodine adsorbed at equilibrium, p is the vapor pressure of iodine, and both k and n are constants. The reported values of n for iodine adsorption onto polymer surface are typically between 0.5 and 0.6 [34,35]. So the temperature determines the amount of iodine adsorbed on the PU at equilibrium, which in turn determines the amount of iodine that diffuses into the foam at equilibrium according to the Fickian model.

3.2.3. Interactions between iodine and the PU foams

The iodine impregnated PU foams were electrically conductive. For PU1 foams impregnated with iodine at 70 °C, the conductivity of the resultant foams is plotted against the iodine concentration in Fig. 3. The conductivity of the PU1 foams with less than 10 wt% of iodine was too low to measure, but the conductivity increased from $\sim 2\times10^{-8}$ to $\sim 5\times10^{-6}$ S/cm as the iodine concentration increased from $\sim$10 to $\sim$130 wt%, which is consistent with a percolation process. Within that concentration range, the conductivity followed a power law relationship

$$\mathrm{Log}(\sigma) = -7.98 + 0.017c^{1.05} \tag{12}$$

where σ is the conductivity in s/cm and c is the iodine concentration in wt%.

Iodine is well known for its ability to form charge–transfer (CT) complexes with many compounds, especially with π-donors, such as electron-rich aromatic compounds [36,37]. This is the mechanism by which iodine doping of extensively conjugated polymers achieves high electrical conductivity [38]. Even for non-conjugated polymers, electrical conductivity can be achieved upon iodine doping, and the conductivity increases with increasing unsaturation, but the conductivity is likely to be ionic [39,40]. Iodine is present in polymers in the form of polyiodides, such as I_3^- and I_5^-, and the relative population of the species is affected by the iodine concentration [41,42]. The Raman spectrum of a PU1 foam with 70 wt% iodine is shown in Fig. 4. The two most prominent peaks are characteristic for the symmetrical I–I stretching vibrations: 109 cm^{-1} for I_3^- and 169 cm^{-1} for I_5^- [41]. The relative intensity of the peaks at 109 and 169 cm^{-1} can be used to estimate the I_3^-/I_5^- ratio [43], which suggests that I_3^- is the major species. It was also observed that the relative population of I_5^- increased with increasing iodine concentration. However, a quantitative study was not carried out.

In the iodine/PU system, a charge–transfer (CT) complex is formed between iodine and the benzene ring from the 2,6-TDI monomer. The CT complex produces physical cross-linking and reduces the mobility of the PU chains, which is manifested as an increase in T_g, see Fig. 5. The T_g increase becomes less significant with increasing iodine concentration, and the T_g asymptotes at higher iodine concentrations, >95 wt% iodine, which may coincide with saturation of the polymer dense regions.

For immiscible binary blends, the ΔC_p of the blend can be expressed as a weighted average of the ΔC_p's of the pure components [44]

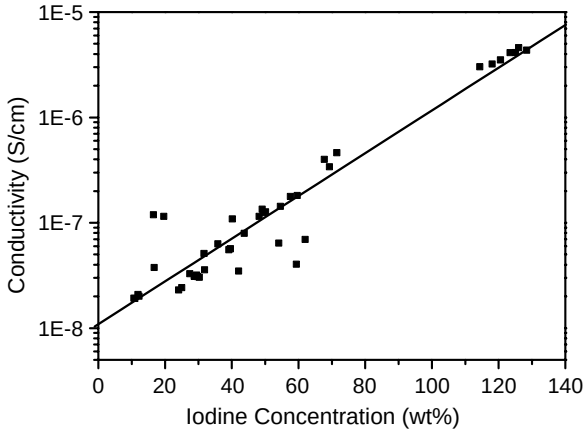

Fig. 3. Electrical conductivity of iodine impregnated PU1 foams versus iodine concentration: foams impregnated with iodine by the iodine sublimation process at 70 °C.

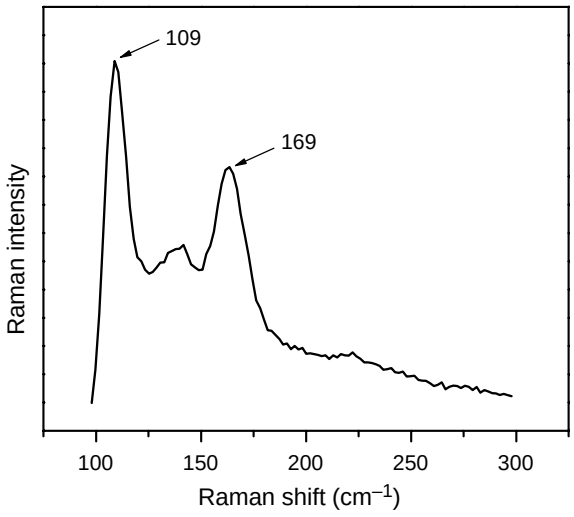

Fig. 4. Raman spectrum of PU1 foam with 70 wt% iodine: foam impregnated with iodine by the iodine sublimation process at 70 °C.

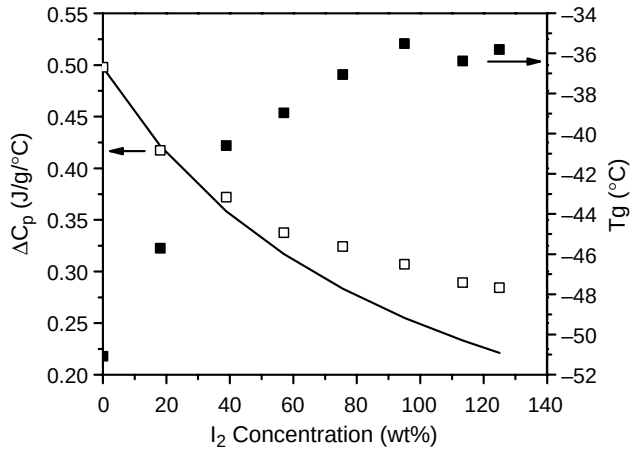

Fig. 5. T_g and ΔC_p at the glass transition measured by DSC versus iodine concentration for PU1 foam impregnated with iodine by iodine sublimation process at 70 °C: (■) T_g measured immediately after iodine sublimation process, (□) ΔC_p at the glass transition measured immediately after iodine sublimation process. The solid line is ΔC_p at the glass transition calculated from Eq. (13).

$$\Delta C_p = \omega_1 \Delta C_{p1} + \omega_1 \Delta C_{p2} \quad (13)$$

where ω_i's are the component polymer weight fractions and ΔC_{pi}'s are the component ΔC_p's at their respective glass transitions. Iodine has no transition in the temperature range investigated. The solid line in Fig. 5 represents the values of ΔC_p at the glass transition for iodine impregnated PU1 foams calculated from Eq. (13). The experimental data show positive deviation from the calculated values, which can be explained as follows. Song et al. [44] treated the glass transition as an Ehrenfest transition of second order and derived an equation which relates ΔC_p at the glass transition with the Flory–Huggins interaction parameter, χ, for miscible binary blends

$$\Delta C_p = \omega_1 \Delta C_{p1} + \omega_1 \Delta C_{p2} + \phi_1 \phi_2 (\chi^l - \chi^g) R/\rho \quad (14)$$

where ϕ_i's are the volume fractions of the component polymers, R is the gas constant, ρ is the density of the blend, and χ^l and χ^g are the interaction parameters for the liquid and the glassy states, respectively. The iodine/PU system can be treated as a miscible binary blend. The CT interaction is exothermic [37] and favored at lower temperature, which implies χ^l, $\chi^g < 0$. Ham studied rigid glasses of solutions of iodine and aromatic hydrocarbons at liquid nitrogen temperature [37]. The equilibrium constants were overwhelming in favor of the presence of a CT complex and the visible absorptions of the CT complex shifted to shorter wavelengths compared with that in liquid state, which indicates a stronger CT interaction in the glassy state, $|\chi^l| < |\chi^g|$. If the same relationship holds for the CT interaction in the iodine/PU system, the excess ΔC_p at the glass transition due to mixing is expected to be positive based on Eq. (14), which is consistent with experimental results.

The temperature dependence of the CT interaction in the iodine/PU system was investigated by annealing the iodine impregnated PU1 foams at different temperatures and then measuring the T_g, as shown in Fig. 6. The iodine impregnated

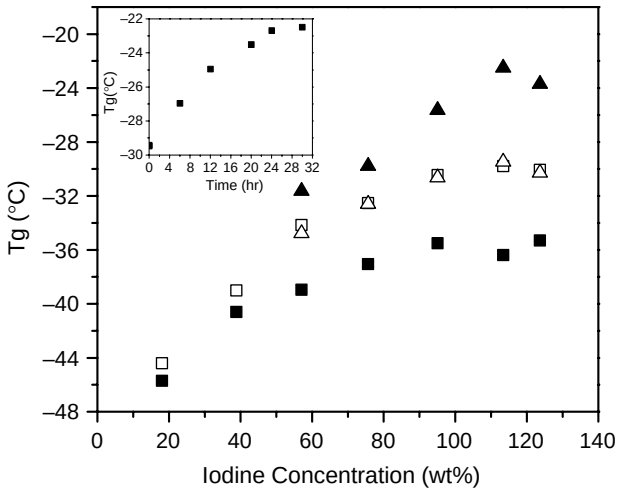

Fig. 6. T_g measured by DSC versus iodine concentration for PU1 foam annealed under different conditions after impregnated with iodine by iodine sublimation process at 70 °C. (■) Condition 1: immediately after iodine sublimation at 70 °C, (□) condition 2: annealed at 25 °C for 7 days after condition 1, (▲) condition 3: annealed at −15 °C for 24 h after condition 2, (△) condition 4: annealed at 25 °C for 24 h after condition 3. The inset shows the increase of T_g with annealing time for a PU1 foam with 113 wt% iodine annealed at −15 °C after condition 2.

PU1 foams were annealed in sealed small vials: there was no detectable weight loss during the annealing experiments. Annealing the iodine impregnated PU1 foams at 25 °C for 7 days after the iodine sublimation process at 70 °C (condition 2 in Fig. 6) resulted in an increase in T_g, especially at high iodine concentrations. The CT interaction equilibrated under this condition, as demonstrated by the invariability of the T_g for longer annealing times at 25 °C. Annealing the iodine impregnated PU1 foams at −15 °C for 24 h after condition 2 (condition 3 in Fig. 6) resulted in a further increase in T_g. However, another 24 h annealing at the higher temperature, 25 °C (condition 4 in Fig. 6) lowered the T_g to the previous value achieved with condition 2. The temperature drop (from 70 to 25, then to −15 °C) may cause iodine to diffuse out of the polymer as the solubility of the iodine in the polymer decreases. The increase in T_g occurred because the CT interaction was favored at the lower temperatures, and the changes of T_g with temperature were reversible.

The change of T_g with temperature was also a kinetic process because of the slow rearrangement of the polymer segments. The inset in Fig. 6 shows the increase in T_g with annealing time for a PU1 foam with 113 wt% iodine annealed at −15 °C after condition 2. It took about 24 h for the iodine impregnated PU1 foam to achieve the new equilibrium after the temperature was lowered from 25 to −15 °C.

The iodine desorption kinetics of the iodine impregnated PU1 foams were measured with a TA Instruments TGA-2950, using a nitrogen atmosphere of flow rate 88 mL/min at 30 °C. The iodine impregnated PU1 foam was annealed at 25 or −15 °C for different periods of time, and then the iodine desorption kinetics was measured by TGA. The amount of iodine desorption was calculated as the percent of desorbed iodine based on the amount of impregnated iodine in the PU1

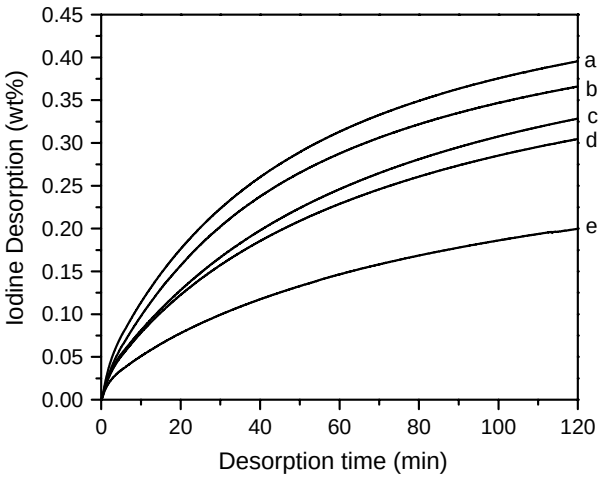

Fig. 7. Iodine desorption kinetics of a PU1 foam with 117 wt% iodine annealed under different conditions after impregnated with iodine by iodine sublimation process at 70 °C: (a) immediately after iodine sublimation at 70 °C, (b) annealed at 25 °C for 6 h, (c) annealed at 25 °C for 12 h, (d) annealed at 25 °C for 24 h, (e) annealed at −15 °C for 24 h.

foams. Lower temperatures and longer annealing times promoted more iodine to complex with the PU, which in turn, should affect the iodine desorption kinetics if it is more difficult to desorb the complexed iodine than the free iodine from PU foams. This conclusion was supported by the iodine desorption data shown in Fig. 7. At 25 °C, the iodine desorption rate decreased with increasing annealing time. For the same annealing time, 24 h, the iodine desorption rate after annealing at −15 °C was significantly lower than that after annealing at 25 °C.

A PU1 foam with 70 wt% iodine was extracted with toluene to isolate the PU1 foam and iodine. The mass of the recovered foam was exactly the same as before the iodine impregnation. FTIR detected no degradation products in the toluene extract. The UV/Vis spectra of the recovered iodine and pure iodine in toluene are compared in Fig. 8. Both spectra show no other absorption peaks besides the two at 500 and 305 nm, which are attributed to iodine and a 1:1 CT complex between iodine and

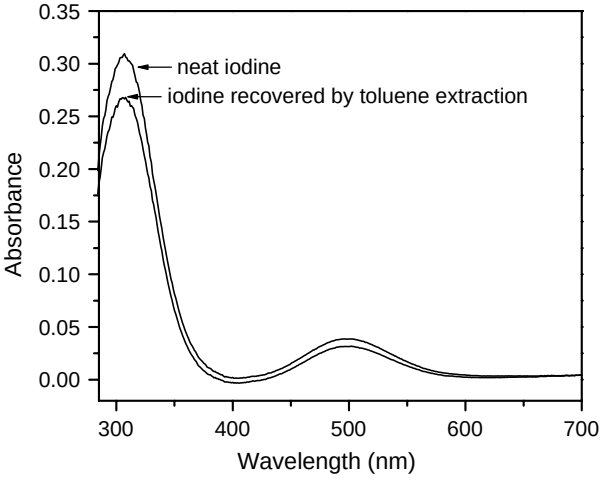

Fig. 8. UV/Vis spectra of iodine recovered by toluene extraction and pure iodine in the solvent of toluene.

toluene, respectively [36,37]. All these results indicate that the complexation between iodine and the PU foam is a reversible process.

3.2.4. Diffusion kinetics

The concentrations of iodine impregnated in three PU foams at three different temperatures are plotted as a function of the square root of time in Fig. 9. For each PU foam the diffusion rate increased with temperature. At each temperature the diffusion rate decreased in the order PU1 > PU2 > PU3, which is consistent with the fact that PU2 had a higher crosslinking

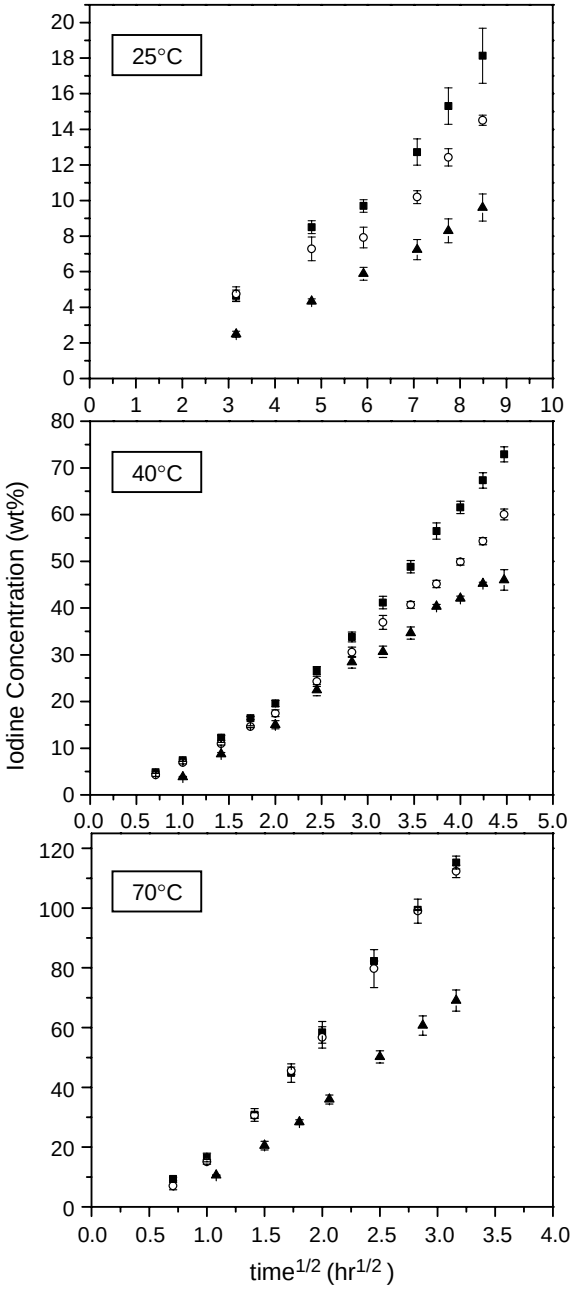

Fig. 9. Iodine concentrations in (■) PU1, (○) PU2, and (▲) PU3 foams as a function of the square root of time using the iodine sublimation process at 25, 40, and 70 °C. The standard deviations (error bars) were calculated from three different foam samples for every data point.

density than PU1 and PU3 contained inorganic fillers. Careful investigation of the diffusion curves shows there was a delay time at the initial stage of diffusion, and then the iodine concentration increased linearly with $t^{1/2}$ up to about 30 wt%. Thereafter, the slopes showed an upward curvature, which indicates a deviation from Fickian diffusion. One possibility for this apparently non-equilibrium behavior is that once the polymer dense phase became saturated with iodine, iodine precipitated within the foam pores. That explanation is consistent with the observation of iodine crystals in some of the samples at high iodine concentrations.

Because equilibrium was not achieved, Eq. (7) was used to estimate M_∞ and D. Because of the composite nature of the foam, i.e. PU fibers and air cells, it is not apparent what value of L should be used; instead, an effective diffusion constant D/L^2 was estimated. The least-squares estimations of M_∞ and D/L^2 obtained at 95% confidence limit are presented in Table 3. For each PU foam, M_∞ increased with increasing temperature, and at each temperature M_∞ decreased in the order PU1 > PU2 > PU3. The latter result is consistent with the higher crosslinking density of PU2 compared to PU1 and the presence of fillers in PU3. The values of D/L^2 were similar (generally within 10%) for the three different foams, which would be expected if this quantity was a material property of the PU phase. D/L^2 did, however, increase with increasing temperature, presumably due to an increase in the diffusivity with temperature.

To gain further insight into the diffusion mechanism, the temperature dependence of diffusivity was further studied by plotting D/L^2 against $1/T$ for the three PU foams, see Fig. 10. The temperature dependence appears to be non-Arrhenius and of a WLF form [30]. Benzene diffusion in natural rubber also displays a similar convex curvature on an Arrhenius plot [19]. The curvature is consistent with Fujita's free-volume diffusion theory [28]. While the WLF nature does not directly imply that the diffusion follows a free-volume dependence, it is usually considered to be a sign of deviation from Fickian diffusion [30]. The diffusion results were fitted to Eq. (9) to further analyze the diffusion mechanism. Because M_∞ and k could not be separated in this case, only the least-squares estimations of n obtained at 95% confidence limit are presented in Table 4. The values of n vary between 0.541 and 0.907, suggesting the diffusion mechanism to be of an anomalous type. Several effects may contribute to this deviation from Fickian diffusion, which will be discussed below.

The delay time at the initial stage may be treated as a violation of the boundary condition. The Fickian model requires that the surface concentration instantaneously attains a constant value C_0 at the start of an experiment. In reality, the surface penetrant concentration may increase rapidly to a constant value, but not instantaneously. Peppas et al. [22] modeled this effect using a variable boundary condition

$$t > 0 \; x = 0, \quad x = 0, \quad x = L \quad C = C_0[1 - \exp(-\beta t)] \qquad (15)$$

Here, β represents a measure of the rate at which the surface equilibrium concentration is attained. This model has demonstrated the delay time at the initial stage of diffusion and its contribution to the overall anomalous diffusion kinetics. The attainment of equilibrium adsorption at the surface of PU phase is also complicated by the two phase nature of the foam. The assumption was that the iodine in the pores equilibrated instantaneously and achieved its vapor pressure in all pores at the same time. This, of course, is not realistic, since the iodine must penetrate a tortuous pathway to reach the interior of the foam. So, a lag time is expected for at least some fraction of the foam.

The early stage of diffusion exhibited typical Fickian behavior as is typical of diffusion in most rubbery polymers. The upward curvature at the late stage of diffusion curve is similar to the typical diffusion behavior in glassy polymers [45], but for a very different reason. Iodine may crosslink the PU chains through CT interaction to reduce the mobility of the PU chains, which was proven by the DSC and iodine desorption kinetics results. This leads to longer relaxation times and the diffusivity D becomes temperature and time dependent. At the late stage of diffusion, the high concentration of iodine in the polymer matrix enhances the crosslinking effect. As a result, the relaxation rate and the diffusion rate become comparable, and the overall diffusion behavior

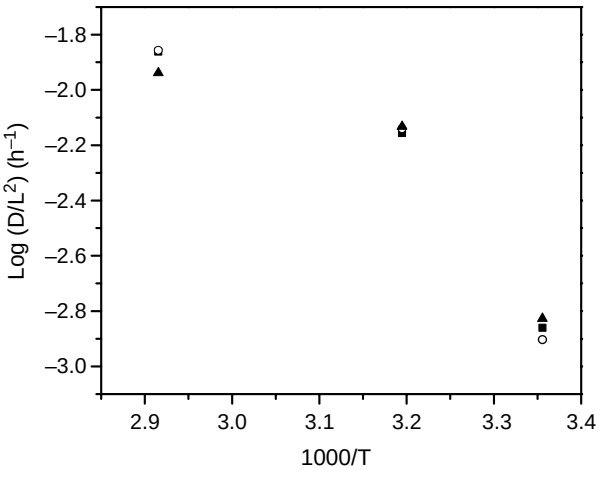

Fig. 10. Temperature dependence of the diffusion constant D/L^2 for (■) PU1, (○) PU2, and (▲) PU3 foams in the iodine sublimation process.

Table 3
Estimated values of M_∞ and D/L^2 from Eq. (7)

Temperature (°C)	M_∞ (wt%)			D/L^2 (h^{-1})		
	PU1	PU2	PU3	PU1	PU2	PU3
25	22.70	19.45	12.03	0.00138	0.00125	0.00149
40	75.78	62.35	52.95	0.00697	0.00724	0.00736
70	122.09	119.11	80.29	0.0138	0.0139	0.0115

Table 4
Estimated values of n from Eq. (9)

Temperature (°C)	PU1	PU2	PU3
25	0.662	0.541	0.678
40	0.750	0.719	0.815
70	0.907	0.855	0.872

becomes anomalous. Alternatively, as was discussed above, the apparent anomalous diffusion may be a consequence of the two phase morphology, where once the dense phase is saturated, iodine condenses within the pores.

The deviation from Fickian diffusion may also be related to polymer swelling. The swelling effect was proven by the swelling ratio data and the morphology changes. Because of the oxidative nature of iodine, the swelling ratios of the iodine impregnated PU foams were only measured for PU1 foams at two iodine concentrations, about 70 and 120 wt%. The swelling ratios were 6.60 ± 0.27 and 18.85 ± 0.54, respectively (the standard derivations were from three measurements). The optical micrographs in Fig. 11 show the typical PU fiber size in neat PU1 foam and PU1 foam with 70 wt% iodine. With the addition of iodine, the average size of PU fibers increased from ca. 70 to 85 μm. Polymer swelling depends on the interactions between penetrant molecules and polymer segments. The interaction between iodine and PU helps iodine diffuse into the interstices of the polymer coils and facilitates swelling of the polymer. The swelling effect may be enhanced by the fact that I_3^- can further complex with I_2 to form the larger I_5^-. During the swelling process, the volume of the polymer matrix increases and the forces holding the polymer segments together become weaker, thereby increasing the pathways for iodine to diffuse. Eventually, the diffusivity becomes concentration dependent as exhibited by the upward curvature of the diffusion curves.

The n values in Table 4 increased with increasing temperature. The temperature dependence of the diffusion mechanism has not been well studied for rubbery polymers, and an explanation based on DSS model [31,32] can be suggested here. The DSS generated by non-uniform polymer swelling may account for the deviation from Fickian diffusion in that the stresses in the polymer are enhanced at higher temperature in rubbery polymers. The value of n decreased from PU1 to PU2, and increased from PU2 to PU3. Those results may also be explained by polymer swelling. With regard to PU2 versus PU1, the higher crosslinking density of PU2 limits the polymer swelling, and thus decreases the concentration dependence of diffusion. For PU3 and PU2, the situation is more complicated. Because PU3 contained inorganic fillers, its equilibrium absorption and swelling decreased. But the existence of a large amount of inorganic fillers already weakened the interchain interactions before the iodine diffusion, and it was easier for iodine to swell the polymer. So the diffusion shows a higher degree of concentration dependence and a higher n value.

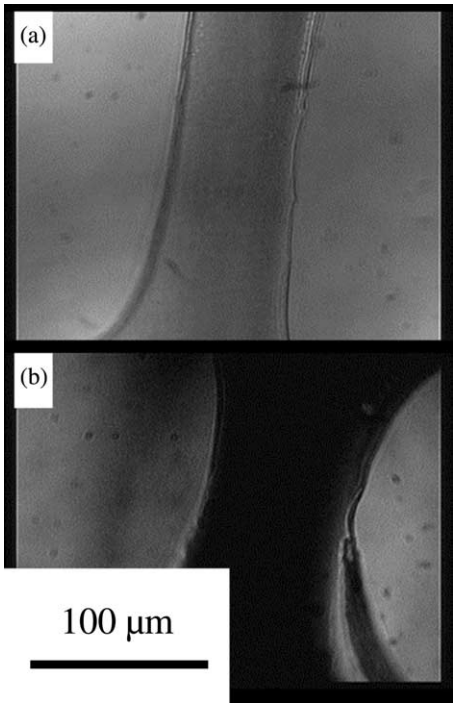

Fig. 11. Optical micrographs of PU fibers of (a) neat PU1 foam and (b) PU1 foam with 70 wt% iodine: foam impregnated with iodine by the iodine sublimation process at 70 °C.

3.3. Iodine solution process

The traditional method of using solvents to incorporate oxidants into host polymers was also investigated. Two solvents, hexanes and toluene were used to impregnate iodine into PU1, PU2, and PU3 foams. There were two reasons to choose those solvents. The first reason is that toluene has a significantly higher affinity for iodine than hexanes because of the CT interaction between toluene and iodine [36]. The maximum concentration of iodine/hexanes solution used was 12 g/L, which is close to the saturated concentration; it took ca. 10 h to complete the dissolution. The maximum concentration of iodine/toluene solution used was 20 g/L and the dissolution was completed in 10 min. The second reason is based on consideration of the solubility parameters of the individual species. The solubility parameter of ether-based PU was calculated to be 17–18 $MPa^{1/2}$, and the solubility parameters of hexanes and toluene are 14.9 and 18.2 $MPa^{1/2}$, respectively [46]. Considering the matching of solubility parameters, toluene is more capable of swelling PU foams than hexanes. This is confirmed by the swelling ratios of three PU foams in hexanes and toluene summarized in Table 5; for each foam the swelling ratio in toluene is significantly larger than that in hexanes. For each solvent the swelling ratio decreased in the order PU1 > PU2 > PU3, but the difference between PU2 and PU3 was not significant. The colors of the iodine/hexanes and iodine/toluene solutions were violet and reddish, respectively. The colors of PU foams containing either solution were yellow or brown, which is similar to the colors of PU foams after the solvents evaporated.

Fig. 12 shows the time for the PU1 foams to achieve absorption equilibrium in iodine/hexanes and iodine/toluene solutions with a concentration of 12 g/L. In hexanes the equilibrium was achieved in less than 45 min, while in toluene the equilibrium was achieved in less than 1 min, which is apparently related to the abilities of the two solvents to swell the foam. Considering the swelling and fast kinetics, the diffusion of iodine into the PU foams using hexanes and toluene is likely to be closer to case II diffusion. In the iodine sublimation process, the iodine distribution in the PU matrix

Table 5
Swelling ratios of PU foams in hexanes and toluene

Foam	Swelling ratio in hexanes	Swelling ratio in toluene
PU1	6.5 (1.0)[a]	26.0 (1.1)
PU2	4.5 (1.2)	20.1 (2.0)
PU3	4.3 (0.3)	19.6 (2.2)

[a] The number in parentheses is the standard deviation of five measurements.

has a concentration gradient from the surface to the core of the PU fibers; in the iodine solution process, the distribution should be more uniform. This was proven by a water sonication experiment of PU1 foams with about 50 wt% iodine concentration from both the iodine sublimation process at 40 °C and the iodine/hexanes solution process. Water is a very polar solvent and has a solubility parameter of 47.9 $MPa^{1/2}$, so water barely swells the foam and only diffuses into a thin layer near the surface of the PU fibers for short immersion times. After water sonication, the iodine concentration of the foam from sublimation process was reduced by 13.24 ± 2.18 wt% and that from hexanes solution process was reduced by 5.90 ± 1.36 wt% (the standard derivations were from three measurements). Although other factors might contribute to this iodine loss, e.g. reverse iodine diffusion from the core to the surface and iodine evaporation during the drying period, the significant reduction of the iodine is believed to be due to the water sonication. The fact that less iodine was removed for the iodine solution process indicates that the solution process produced a more uniform distribution of iodine in the PU matrix.

In Fig. 13, the iodine sorption data at equilibrium are plotted against the concentration of the iodine/hexanes or iodine/toluene solution used for iodine impregnation. The linear relationship implies that the distribution of iodine between the solvent and the PU foam followed a distribution law which states that if a substance soluble in two immiscible solvents is added to a mixture of the two solvents, the third substance distributes itself between the two solvents so that the ratio of the concentration in one solvent to the concentration in the second solvent remains constant at constant temperature. The

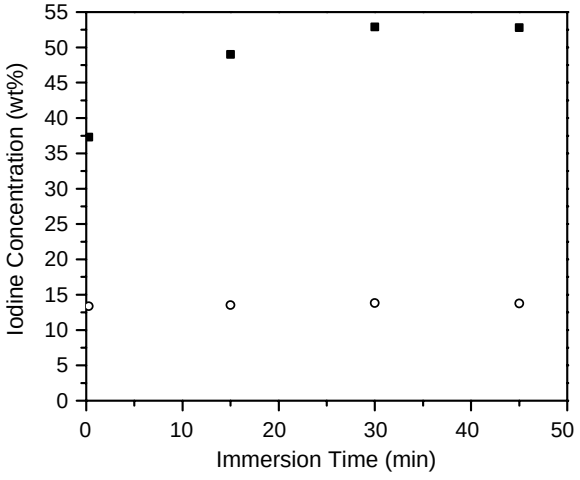

Fig. 12. Sorption of iodine versus time by PU1 foam immersed in (■) iodine/hexanes and (○) iodine/toluene solutions with a concentration of 12 g/L. The immersion time for the fist data point is 0.5 min.

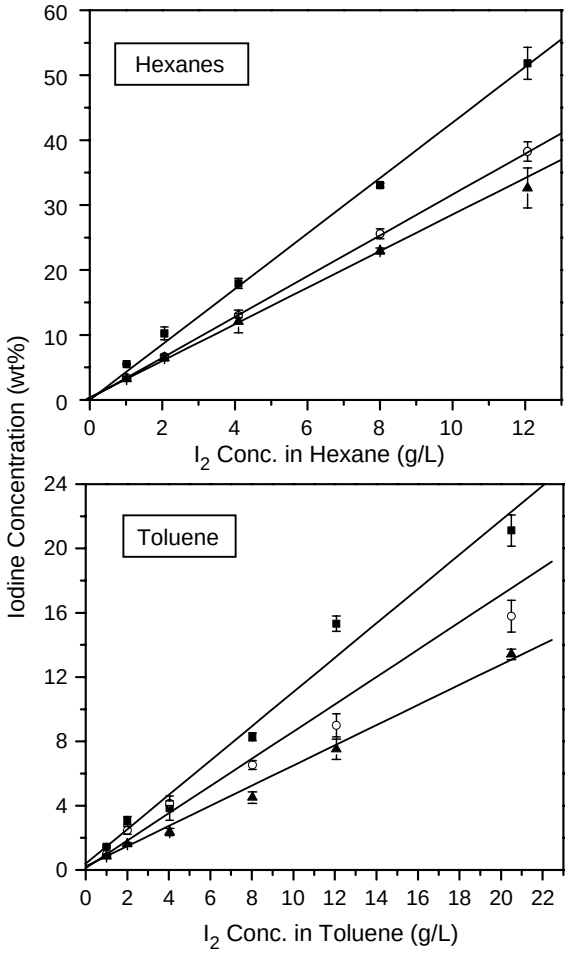

Fig. 13. Sorption of iodine versus iodine concentration in the solvent of hexanes or toluene for (■) PU1, (○) PU2, and (▲) PU3 foam. The standard deviations (error bars) were calculated from three measurements.

constant ratio is termed the distribution coefficient [47]. The distribution law is usually concerned with the solvent extraction process. The crosslinked PU foam in this case may be considered a viscous solvent that is immiscible with hexanes or toluene. The concentrations of iodine in the solvents at equilibrium were calculated from a mass balance of the iodine. The distribution coefficients, K_i, defined as the ratio of the concentration of iodine in the PU foam to the concentration of iodine in the solvent at equilibrium, for the three foams are summarized in Table 6. For each solvent, K_i decreased in the order PU1 > PU2 > PU3, because the higher crosslinking density of PU2 and the inorganic fillers of PU3 limited their ability to absorb iodine. For each foam, the K in toluene was significantly lower than that in hexanes, which is in agreement with the higher affinity of toluene for iodine compared with hexanes. The ratio of K_i in hexanes (K_1) and toluene (K_2) for each foam is also listed in Table 6. The ratios for PU1 and PU2 are the same, but different from that for PU3. K can be viewed as a measure of the ability of a solvent to compete for a solute against another solvent, and then the ratio can be viewed as the comparison of the abilities of hexanes and toluene to compete for the same solute (iodine) against the same solvent (PU

Table 6
Distribution coefficients of iodine between the PU foam and the solvent

Foam	K_1 (in hexanes)	K_2 (in toluene)	K_1/K_2
PU1	3.96	1.07	3.70
PU2	3.14	0.85	3.69
PU3	2.82	0.63	4.48

foam). So, it is not a coincidence that the ratios are the same for PU1 and PU2. The reason for PU3 to have a different ratio is probably that the inorganic fillers make the mechanism more complicated.

3.4. Iodine sorption by MF foams

The MF foam was used in both iodine impregnation processes. In the sublimation process, the iodine diffusion lasted for 4 h at 70 °C and less that 0.1 wt% of iodine was adsorbed on the surface of the foam. That iodine quickly evaporated after the foam was removed from the desiccator. In the solution process, almost no iodine was absorbed by the foam after it was squeezed to eliminate the solution. Even without squeezing the foam, iodine evaporated almost as fast as the solvents and no absorption by the foam was achieved. An interesting observation, however, was that the MF foam containing the iodine solution still exhibited the color of the solution used, violet for hexanes and reddish for toluene. Considering the color changes of the iodine impregnation in PU foams, the similarity of the colors of the MF foams and the solution used to impregnate them with iodine is probably due to a lack of interactions between iodine and MF foams.

Fig. 14 shows the simplified chemical structures of PU and MF foams. The major electron donor in PU is the benzene ring from TDI, while the major electron donor in MF is the conjugated structure of s-triazine and tertiary amines from melamine. In heterocyclic chemistry, the substitution of a ring carbon by a nitrogen causes reduced aromatic stability, increased π-deficiency and less π-donor character [48]. To extrapolate from benzene through pyridine to diazine and then to triazine, the compounds become weaker electron donors in the order benzene > pyridine > diazine > triazine and behave more as an n-donor on interaction with an electron acceptor such as iodine. The CT complex between iodine and s-triazine could not even be detected [49]. The structural difference of MF compared with PU may explain the poor ability of MF foams to absorb iodine, but the fact that MF foams could not absorb iodine at all was surprising.

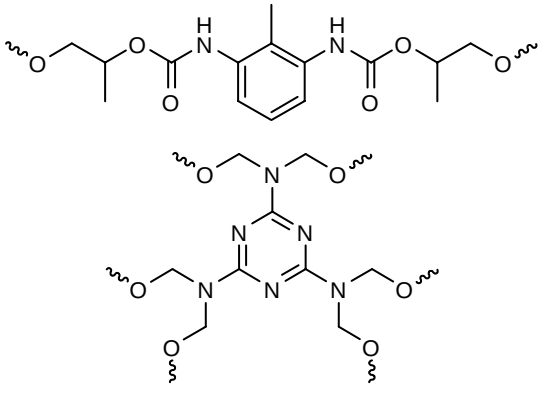

Fig. 14. Chemical structures of PU foam and MF foam.

4. Conclusions

The iodine sorption by PU and MF foams using iodine sublimation and iodine solutions was investigated. In the sublimation process, the diffusion kinetics exhibited anomalous diffusion behavior, which was believed to be due to the transient of the initial adsorption process, the charge–transfer interaction between iodine and PU, and/or polymer swelling. The polymer swelling also accounted for the effects of temperature and PU foam characteristics on the diffusion behavior. In the iodine solution process, the absorption equilibrium was achieved in a short time because of the ability of solvents to swell the PU foams, and a more uniform distribution of iodine in the polymer matrix was obtained. The equilibrium absorption in the PU foams followed a distribution law and the distribution coefficients varied depending on the affinity of the solvent for iodine. The MF foam achieved no iodine absorption in both processes because of its poor ability to interact with iodine.

For the iodine sorption by a host polymer, kinetics dictate how long it takes to achieve equilibrium and how iodine is distributed in polymer matrix; thermodynamics determines how much iodine may be incorporated into polymers. Both aspects greatly depend on the interactions between polymers, iodine and solvents. The results here may provide some guidelines to adopt an optimum oxidant impregnation process to achieve the desired amount and distribution of oxidants in a host polymer and, thus, the desired PPy/polymer blends after in situ polymerization of pyrrole.

Acknowledgements

G.A. Sotzing would like to acknowledge the National Science Foundation DMR 0502928 for partial support of this work.

References

[1] Ramani R, Ranganathaiah C. Polym Int 2001;50(2):237–48.
[2] Harogoppad SB, Aminabhavi TM. Macromolecules 1991;24(9):2598–605.
[3] Scheichl R, Klopffer MH, Benjelloun-Dabaghi Z, Flaconneche B. J Membr Sci 2005;254(1–2):275–93.
[4] Skotheim TA, Elsenbaumer RL, Reynolds JR, editors. Handbook of conducting polymers. 2nd ed; 1997 [revised and expanded].
[5] Chandrasekhar P. Conducting polymers, fundamentals and applications: a practical approach; 1999.
[6] Miasik JJ, Hooper A, Tofield BC. J Chem Soc Faraday Trans 1: Phys Chem Condens Phases 1986;82(4):1117–26.
[7] De JMC, Fu Y, Weiss RA. Polym Eng Sci 1997;37(12):1936–43.
[8] Fu Y, Weiss RA, Gan PP, Bessette MD. Polym Eng Sci 1998;38(5):857–62.
[9] Ishizu K, Honda K, Kanbara T, Yamamoto T. Polymer 1994;35(22):4901.
[10] Ishizu K, Honda K, Saito R. Polymer 1996;37(17):3965.

[11] Lafosse X. Synth Met 1995;68(3):227.
[12] Zoppi RA, Felisberti I, De Paoli MA. J Polym Sci Part A: Polym Chem 1994;32(6):1001–8.
[13] Fu Y, Palo DR, Erkey C, Weiss RA. Macromolecules 1997;30(24): 7611–3.
[14] Shenoy SL, Kaya I, Erkey C, Weiss RA. Synth Met 2001;123(3):509–14.
[15] Shenoy SL, Cohen D, Weiss RA, Erkey C. J Supercrit Fluids 2004;28(2–3):233–9.
[16] Shenoy SL, Cohen D, Erkey C, Weiss RA. Ind Eng Chem Res 2002;41(6): 1484–8.
[17] Wang Y, Sotzing GA, Weiss RA. Chem Mater 2003;15(2):375–7.
[18] Nielsen LE, Landel RF. Mechanical properties of polymers and composites. 2nd ed; 1994.
[19] Crank J, Park GS, editors. Diffusion in polymers; 1968.
[20] Meares P. Polymers: structure and bulk properties; 1965.
[21] Barrer RM. Nature 1937;140:106–7.
[22] Peppas NA, Brannon-Peppas L. J Food Eng 1994;22(1–4):189.
[23] Webb AG, Hall LD. Polymer 1991;32(16):2926.
[24] Alfrey JT, Gurnee EF, Lloyd WG. J Polym Sci, Part C: Polym Symposia 1966;12:49–261.
[25] Thomas NL, Windle AH. Polymer 1980;21(6):613.
[26] Sammon C, Yarwood J, Everall N. Polymer 2000;41(7):2521.
[27] Aminabhavi TM, Khinnavar RS. Polymer 1993;34(5):1006–18.
[28] Fujita H. Fortschr Hochpolymer Forsch 1961;3(1):1–47.
[29] Schneider NS, Moseman JA, Sung NH. J Polym Sci, Part B: Polym Phys 1994;32(3):491–9.
[30] Pant PVK, Boyd RH. Macromolecules 1993;26(4):679–86.
[31] Crank J. J Polym Sci 1953;11:151–68.
[32] Sanopoulou M, Petropoulos JH. Polymer 1997;38(23):5761–8.
[33] Gillespie LJ, Fraser LHD. J Am Chem Soc 1936;58:2260–3.
[34] Saeed MM, Ahmed M, Ghaffar A. Sep Sci Technol 2003;38(3):715–31.
[35] Singhal JP, Ray AR. Trends Biomater Artif Organs 2002;16(1):46–51.
[36] Benesi HA, Hildebrand JH. J Am Chem Soc 1949;71:2703–7.
[37] Ham J. J Am Chem Soc 1954;76:3875–80.
[38] Chiang CK, Fincher Jr CR, Park YW, Heeger AJ, Shirakawa H, Louis EJ, et al. Phys Rev Lett 1977;39(17):1098–101.
[39] Auten KL, Petrovic ZS. J Polym Sci, Part B: Polym Phys 2002;40(13): 1316–33.
[40] Jendrasiak GL, Madison GE, Smith R, McIntosh TJ. Biosens Bioelectron 1992;7(4):291.
[41] Pannell KH, Imshennik VI, Maksimov YV, Il'ina MN, Sharma HK, Papkov VS, Suzdalev IP. Chem Mater 2005;17(7):1844–50.
[42] Murthy NS. Macromolecules 1987;20(2):309–16.
[43] Tanaka J, Mizuno M. Bull Chem Soc Jpn 1969;42(7):1841–52.
[44] Song M, Hourston DJ, Pollock HM, Hammiche A. Polymer 1999;40(17): 4763–7.
[45] Berens AR, Hopfenberg HB. Polymer 1978;19(5):489.
[46] Brandrup J, Immergut EH, editors. Polymer handbook. 4th ed; 1998.
[47] Vogel AI, Furniss BS, Hannaford AJ, Rogers V, Smith PWG, Tatchell AR. Vogel's textbook of practical organic chemistry; 1978.
[48] Katritzky AR, Pozharskii AF, editors. Handbook of heterocyclic chemistry. 2nd ed; 2000.
[49] Krishna VG, Chowdhury M. J Phys Chem 1963;67:1067–9.